SoftwareX 9 (2019) 299–307

Contents lists available at ScienceDirect

SoftwareX

journal homepage: www.elsevier.com/locate/softx

Original software publication

FMC—Earthquake focal mechanisms data management, cluster and classification

José A. Álvarez-Gómez

Department of Geodynamics, Stratigraphy and Palaeontology; Faculty of Geology; Complutense University of Madrid, C/ José Antonio Novais, 12. 28040 Madrid, Spain

ARTICLE INFO

Article history:
Received 5 November 2018
Received in revised form 26 March 2019
Accepted 26 March 2019

Keywords:
Earthquake
Focal mechanism
Clustering

ABSTRACT

Seismicity is frequently used to deduce the tectonics of a region. The study of earthquakes as a tectonic component, seismotectonics, has grown as one of the key research areas on active tectonics, especially from the analysis of earthquake focal mechanisms. FMC computes the different earthquake parameters that can be obtained from focal mechanism data, classifies the rupture type of each focal mechanism, performs a clustering analysis of the data if required by the user, outputs the parameters in different formats and generates a classification diagram from the input data.

Code metadata

Current code version	v1.3
Permanent link to code/repository used for this code version	https://github.com/ElsevierSoftwareX/SOFTX_2018_227
Legal Code License	GPL v3
Code versioning system used	git
Software code languages, tools, and services used	python
Compilation requirements, operating environments & dependencies	Python modules matplotlib, NumPy, sys, argparse, os, SciPy
If available Link to developer documentation/manual	https://github.com/Jose-Alvarez/FMC
Support email for questions	jaag@ucm.es

1. Motivation and significance

The first earthquake focal mechanism determination methods, based on P wave first motion polarities, were developed in the first half of the 20th century, more specifically in Japan where a dense seismic network was available [1–5]. Since 1960, computers have allowed the numerical determination of fault-plane solutions with different, more robust, methods [e.g. 6–8]. In parallel with the development of modern seismology, the theory of plate tectonics changed the way geologists understand the Earth. Consequently, the study of earthquakes related to plate tectonics was developed at the same time, the basic concepts of seismotectonics and the lithospheric deformation were established [e.g. 9–12].

Since the 70s, earthquake focal mechanisms started to be computed in a systematic way and global catalogues of focal mechanisms. Because of the continuous increase in data available, we need new tools to analyse it systematically. In order to represent focal mechanism populations, Frohlich and Apperson [13] proposed a diagram to visualize focal mechanism data as a function of the rupture type. This representation is popular and widely used in seismotectonics to represent the focal mechanisms of the study area [e.g. 14–19]. However, since it is significantly distorted towards the lower corners [20], Kagan [21] used the Kaverina equal-area projection [22] to avoid them. The difference between both diagrams is similar to that found between gnomonic and Lambert azimuthal equal-area projections (see the FMC manual for more details).

The aim of the FMC program is to provide a simple but powerful tool to manage focal mechanism data, classify the events according to the earthquake double-couple (DC) rupture type, and optionally perform a clustering analysis and plot a classification diagram based on DC characteristics. The combination of these functionalities allows a deeper analysis of earthquake ruptures

E-mail address: jaalvare@ucm.es.

https://doi.org/10.1016/j.softx.2019.03.008

Table 1
Focal mechanisms inversion and analysis software.

Software	Reference
Single focal mechanism inversion and plotting programs	
FOCMEC	Snoke, 1984 [23]
EARTHWORM	Johnson et al. 1995 [24]
Coral tools	Creager 1997 [25]
Rake	Louvari & Kiratzi, 1997 [26]
Geotouch	Lees, 2000 [27]
FPSPACK	Gasperini & Vannucci [28]
Dishansh 2005	Srivastava et al. 2006 [29]
MIRONE	Luis, 2007 [30]
3DFM	Labay & Haeussler, 2007 [31]
Earthquake Focal Mechanism	Scherbaum et al. 2009 [32]
SeisComP	Hanka et al. 2010 [33]
MoPaD	Krieger & Heimann, 2012 [34]
Computer programs in seismology	Herrmann, 2013 [35]
focalmech	Conder, 2017 [36]
Grond (Pyrocko)	Heimann et al. 2018 [37]
bb	CERI, 2019 [38]
Focal Mechanisms	Helffrich, 2019 [39]
psmeca, pscoupe (GMT)	Patau, 2019 [40]
PyTDMT (ObsPy)	Bernardi, 2019 [41]
Focal mechanisms population analysis and plotting programs.	
Geotouch	Lees, 2000 [27]
EQuakes	Lister, 2010 [42]
TFMtools	Khalil & Al-Arifi, 2018 [43]

in a region, providing greater insight into the tectonic processes responsible for the seismicity.

Other tools have been developed for focal mechanism analysis and management that are complimentary to FMC. Some of them are used exclusively in the process of seismological data to obtain the focal mechanism and/or its plotting on a singular basis ("beach-ball" representation). In Table 1, a number, although not all, of these programs are listed.

In order to represent and perform a statistical analysis of populations of focal mechanisms, different approaches and algorithms have been proposed. In Table 1, some published programs are shown. Other authors have proposed different algorithms and methods although no distributable specific software is available [e.g. 21,22,44–48]. Some of them are based on the Frohlich and Apperson ternary diagram for DC tensors [13], while others are based on the Hudson source classification [49]. The clustering analysis of focal mechanism populations has also been explored, but again, no specific software has been developed [e.g. 50–54].

To date, FMC has been used in several research projects and publications analysing the seismotectonics of areas [55–64] or seismic series [65–68]. The software is normally used to classify the events according to rupture type in an area or seismic series, which used to be accompanied by a diagram showing DC classification, and then an additional analysis or modelling is performed. Recently added capabilities to the software, such as extended plotting options and clustering analysis, are yet to be explored and imply a qualitative step forward in seismotectonic analysis.

2. Software description

The program has been designed with the modularity and versatility of the classical UNIX-like tools. It is called from the command line and can be easily integrated into shell scripts (*NIX systems) or batch files (DOS/Windows systems).

FMC was originally programmed in Python 2.7.3 using several common Python libraries: sys, argparse, os, NumPy (version 1.14 or higher) and matplotlib. Since version 1.3, FMC also works on Python 3. The core functions for focal mechanism data manipulation adapt some FORTRAN subroutines from Gasperini & Vannucci [28].

2.1. Software functionalities

The program input and outputs can be performed by means of ASCII files or using standard input (or redirection "<"), standard output (screen or redirection ">") and pipes ("|"). By default, FMC will read the input and write the output as a Harvard CMT (psmeca formatted) ASCII file. The input format can be changed by the program option modifier "-i", while the output format is selected with the "-o" modifier.

Data should be entered into the program using one of the three focal mechanism formats of the GMT (Generic Mapping Tools) package [69]. The formats are the Harvard CMT convention, the two nodal planes old Harvard CMT format for psmeca, and the single nodal plane Aki and Richards [70] convention. The former is a complete format that can be downloaded directly from the Global CMT site (http://www.globalcmt.org/), while the latter is the simplest way to incorporate earthquake rupture data.

Optionally, FMC will produce a Kaverina-type DC classification diagram (with the program option "-p"). FMC uses matplotlib libraries and can generate figures in different formats (emf, eps, jpeg, jpg, pdf, png, ps, raw, rgba, svg, svgz, tif, tiff). The format is determined automatically from the plot file name extension.

The diagram is based on the Kaverina [22] projection technique, used also by Kagan [21], but it incorporates a DC classification similar to the geological conceptual classification of faults. The earthquakes are classified into seven types according to the values of the P, T and B Centroid Moment Tensor axes following a simple algorithm and are opportunely represented on the Kaverina diagram (Fig. 1). This classification is very similar to the one used by Johnston et al. [71–73]. Currently, FMC produces only DC classification diagrams. For source-type classification diagrams, the reader can refer to recent works on the subject [48,74,75].

Common practice when working with seismic moment tensors requires decomposition of the tensor, which is iso-deviatoric following the procedure implemented by Gasperini and Vanucci [28]. The compensated linear vector dipole ratio, fclvd, which measures how different a source is from a "pure" double couple, is computed as defined by Frohlich and Apperson [13]. In order to obtain the nodal planes of the double couple, the orientation of the main axes (P, B, T) is computed from the deviatoric moment tensor (the P- and T-axis being the same for the DC and the CLVD components). Nodal plane orientations and slip vectors are obtained geometrically from the P- and T-axis. Inverse computation can also be performed, obtaining the P-, T- and B-axis orientations from the nodal planes (in fact only one nodal plane is necessary as both are mutually orthogonal and kinematically constrained). In this case, the moment tensor obtained is a pure DC with fclvd $= 0$.

FMC implements the hierarchical agglomerative clustering algorithms from SciPy to group data. The advantages of these algorithms are their versatility, as the user can choose between a number of metrics and grouping methods, their capacity to automatically select a minimum number of clusters without a priori estimation, and their potential to work with different parameters with different scales and strong different populations in clusters.

2.2. Available command line switches

The program uses different options or flags controlling the following aspects: (i) input formats, (ii) output formats, (iii) plotting options and (iv) clustering options. Additionally there is the common "-v" verbose option for information.

2.2.1. Input

FMC input can be given as an ASCII file or as standard input, from a pipe ("|") or a redirection ("<"). The following codes are then equivalent:

```
FMC.py input-file.dat
cat input-file.dat | FMC.py
FMC.py < input-file.dat
```

If no input is given, then FMC will show the on-screen help.

The input format is specified with the optional flag "-i", and the possible values are:

CMT Harvard Centroid Moment Tensor (by default):

[longitude, latitude, depth, mrr, mtt, mff, mrt, mrf, mtf, Exponent (dyn.cm), X plot, Y plot (for GMT), ID]

AR Aki and Richards one plane convention:

[longitude, latitude, depth, strike, dip, rake, magnitude (Mw), X plot, Y plot (for GMT), ID]

P Focal mechanism both nodal planes:

[longitude, latitude, depth, strike A, dip A, rake A, strike B, dip B, rake B, Scalar seismic moment mantissa, Exponent (dyn.cm), X plot, Y plot (for GMT), ID]

2.2.2. Output

FMC output format can be selected among the following options with the flag "-o":

CMT Harvard Centroid Moment Tensor (psmeca compatible):

[longitude, latitude, depth, mrr, mtt, mff, mrt, mrf, mtf, Exponent (dyn.cm), X plot, Y plot (for GMT), ID, TYPE]

P Focal mechanism both nodal planes (psmeca compatible):

[longitude, latitude, depth, strike A, dip A, rake A, strike B, dip B, rake B, Scalar seismic moment mantissa, Exponent (dyn.cm), X plot, Y plot (for GMT), ID, TYPE]

AR Focal mechanism one plane (psmeca compatible):

[longitude, latitude, depth, strike, dip, rake, magnitude (Mw), X plot, Y plot (for GMT), ID, TYPE]

K Kaverina diagram position for plotting outside FMC:

[X Kaverina diagram, Y Kaverina diagram, Mw, Depth, ID, TYPE]

ALL All parameters obtained:

[longitude, latitude, depth, mrr, mtt, mff, mrt, mrf, mtf, Exponent (dyn.cm), Scalar seismic moment (dyn.cm), Mw, strike A, dip A, rake A, strike B, dip B, rake B, Slip trend A, Slip plunge A, Slip trend B, Slip plunge B, P trend, P plunge, B trend, B plunge, T trend, T plunge, fclvd, isotropic component, X Kaverina diagram, Y Kaverina diagram, ID, TYPE]

CUSTOM In case you need any focal mechanism parameters in any order you can use the CUSTOM option and give the requested parameters using the flag "-of". The output parameters need to be listed separated by commas. The accepted parameter names are listed below and can be seen on the terminal using FMC.py -helpFields

Table 2
Parameter names used in FMC.

Code	Parameter
lon	longitude
lat	latitude
dep	depth
mrr	mrr centroid moment tensor component
mtt	mtt centroid moment tensor component
mff	mff centroid moment tensor component
mrt	mrt centroid moment tensor component
mrf	mrf centroid moment tensor component
mtf	mtf centroid moment tensor component
mant	mantissa of the seismic moment tensor
expo	exponent of the seismic moment tensor
Mo	Scalar seismic moment
Mw	Moment (or Kanamori) magnitude
posX	X plotting position for GMT psmeca
posY	Y plotting position for GMT psmeca
ID	ID of the event
clas	Focal mechanism rupture type
strA	Strike of nodal plane A
dipA	Dip of nodal plane A
rakeA	Rake of nodal plane A
strB	Strike of nodal plane B
dipB	Dip of nodal plane B
rakeB	Rake of nodal plane B
slipA	Slip sense of plane A
plungA	Plunge of slip vector of plane A
slipB	Slip sense of plane B
plungB	Plunge of slip vector of plane B
trendp	Trend of P axis
plungp	Plunge of P axis
trendb	Trend of B axis
plungb	Plunge of B axis
trendt	Trend of T axis
plungt	Plunge of T axis
fclvd	Compensated linear vector dipole ratio
iso	Moment tensor isotropic component
x_kav	x position on the Kaverina diagram
y_kav	y position on the Kaverina diagram

2.2.3. Plot

FMC uses several flags to customize the plot.

-p This flag activates the plotting. It must be followed by the name of the figure file that will be produced. The name chosen for the file (without the extension) is used as a title for the plot.

-pc With this flag the user specifies the parameter that is used to fill the symbols. A colour palette is produced with the selected parameter value range.

-pa This flag is used to annotate the symbols with a certain parameter.

-pg If present, the program will plot grid-lines with the specified angular spacing on the diagram plot (10° by default).

With -pc and -pa, the parameters must be given with their corresponding internal name as listed in Table 2.

2.2.4. Clustering

With the increment of focal mechanisms available for studying the seismotectonics of an area or a seismic series, the need for tools to perform statistical analyses has grown. The clustering analysis is now a common statistical tool that allows a large amount of different clustering strategies to be adapted to any problem.

I have chosen to include hierarchical clustering (connectivity-based clustering) as a clustering algorithm in FMC. Although other algorithms can work well with focal mechanisms, hierarchical

clustering presents a suite of linkage methods and distance metrics that makes this algorithm very versatile and users can choose which method and metric is better suited to their specific tasks. This clustering algorithm groups every event into a cluster and consequently every focal mechanism is used and incorporated in the analysis. Other alternative clustering algorithms will be included in future releases of FMC after they have been tested.

The parameters for the clustering are passed by several optional flags. If any of the following flags is given in the command line FMC will perform the clustering analysis using some default options if needed. When a clustering analysis is done, by default FMC will shade the symbols in the diagram using the cluster number unless a different parameter is stated with -pc flag.

-cm Method to be used in the clustering analysis.[1]

The options are:

single single/minimum/nearest

$$d(u, v) = \min(dist(u[i], v[j]))$$

complete complete/max/farthest point

$$d(u, v) = \max(dist(u[i], v[j]))$$

average average/UPGMA

$$d(u, v) = \sum_{ij} \frac{d(u[i], v[j])}{(|u| * |v|)}$$

weighted weighted/WPGMA

$$d(u, v) = (dist(s, v) + dist(t, v))/2$$

centroid centroid/UPGMC [default]

$$dist(s, t) = \|c_s - c_t\|_2$$

where c_s and c_t are the centroids of clusters s and t, respectively. When two clusters s and t are combined into a new cluster u, the new centroid is computed over all the original objects in clusters s and t. The distance then becomes the Euclidean distance between the centroid of u and the centroid of a remaining cluster v in the forest.

median median/WPGMC, assigns $d(s, t)$ like the centroid method. When two clusters s and t are combined into a new cluster u, the average of centroids s and t give the new centroid.

ward Ward variance minimization algorithm.

$$d(u, v) = \sqrt{\frac{|v| + |s|}{T} d(v, s)^2 + \frac{|v| + |t|}{T} d(v, t)^2 - \frac{|v|}{T} d(s, t)^2}$$

where u is the newly joined cluster consisting of clusters s and t, v is an unused cluster in the forest, $T = |v| + |s| + |t|$, and $|*|$ is the cardinality of its argument.

Methods "centroid", "median" and "ward" are correctly defined only if Euclidean pairwise metric is used. When analysing rupture characteristics (for example the position on the Kaverina diagram) the choices of "centroid" or "median" linkage methods are reasonable. When analysing the spatial position of the events, for example in a seismic series, maybe the "single" or "complete" linkage methods are better suited.

-ce Metric used to measure distances between events parameters.[2] These metrics work with non-Boolean vectors.

By default FMC uses Euclidean distance, which is a reasonable choice when working with numerical values on the same units. For example, when using only the epicentral position of the events, or the position of the events in the Kaverina diagram (rupture type) or any other clustering approximation using a limited number of parameters in a common physical magnitude and unit. When performing more complex clustering analysis, with parameters such as slip direction, epicentral position and magnitude, the Euclidean metric will produce anomalous results, as the parameters are in different units and magnitudes. To avoid this problem, the different parameters can be normalized so they can be compared. The Mahalanobis metric, for example, normalizes each parameter with its covariance matrix, so they can be used together.

When analysing seismotectonic data in areas, a useful approximation is to split the clustering into several steps, for example, performing first a rupture-type clustering and then spatial clustering or vice versa, rather than mixing all the parameters in one analysis.

braycurtis The Bray–Curtis distance between two points u and v is

$$d(u, v) = \frac{\sum_i |u_i - v_i|}{\sum_i |u_i + v_i|}$$

canberra The Canberra distance between two points u and v is

$$d(u, v) = \sum_i \frac{|u_i - v_i|}{|u_i| + |v_i|}$$

chebyshev The Chebyshev distance between two n-vectors u and v is the maximum norm-1 distance between their respective elements. More precisely, the distance is given by

$$d(u, v) = \max_i |u_i - v_i|$$

cityblock City block or Manhattan distance between the points.

correlation Correlation distance between vectors u and v. This is

$$1 - \frac{(u - \bar{u}) \cdot (v - \bar{v})}{\|(u - \bar{u})\|_2 \, \|(v - \bar{v})\|_2}$$

cosine Cosine distance between vectors u and v,

$$1 - \frac{u \cdot v}{\|u\|_2 \, \|v\|_2}$$

euclidean Distance between m points using Euclidean distance (2-norm). [Default]

hamming Normalized Hamming distance, or the proportion of those vector elements between two n-vectors u and v which disagree.

jaccard Jaccard distance between the points. Given two vectors, u and v, the Jaccard distance is the proportion of those elements $u[i]$ and $v[i]$ that disagree.

[1] The details on the clustering algorithms shown in this section are taken from the SciPy documentation.

[2] The details on the clustering algorithms shown in this section are taken from the SciPy documentation.

mahalanobis The Mahalanobis distance between two points u and v is

$$\sqrt{(u-v)(1/V)(u-v)^T}$$

where $1/V$ is the inverse covariance matrix.

minkowski Distances using the Minkowski distance $\|u-v\|_p$ (p-norm) where $p \geq 1$.

seuclidean Standardized Euclidean distance. The standardized Euclidean distance between two n-vectors u and v is

$$\sqrt{\sum (u_i - v_i)^2 \div V[x_i]}$$

V is the variance vector; $V[i]$ is the variance computed over all the i'th components of the points. It is automatically computed.

sqeuclidean Squared Euclidean distance $\|u-v\|_2^2$ between the vectors.

-cn A priori number of clusters to obtain.

If it is zero or not present, the number of clusters is automatically computed using the Elbow method. This method uses the percentage of variance explained as a function of the number of clusters; when the increase in the number of clusters does not improves the percentage of variance explained the number of clusters is set.

-ci Parameters used to perform the cluster analysis.

By default, FMC uses the position (X and Y coordinates) on the Kaverina diagram, which is a proxy for the principal moment tensor axes plunges and related to the Kagan minimum rotation angle [21]. If the parameters given are not in the same physical magnitude and unit, the Euclidean distance is not appropriate and a different metric should be used. In these cases, the Mahalanobis distance is a good choice, as it is equivalent to the Euclidean distance in the transformed space, using the covariance matrix of each parameter.

The parameters to be used for the clustering analysis must be given with their corresponding internal name as listed in Table 2.

The clustering algorithm is the most demanding on computing capacities. In order to perform the clustering, pairwise distances between points are computed by means of numpy arrays with dimensions (n(n-1)/2). Taking into account that numpy uses the double array data type with size 8 bytes, to perform a clustering analysis with the complete GlobalCMT [76] catalogue (∼ 30000 events), a computer with at least 3.3 Gbytes of RAM is needed.

3. Examples of use

- Obtaining nodal planes from moment tensor
  Command:
  `echo -2.54 37.09 12 -3.4669 -2.0652 5.5321 6.2368 -1.8004 -5.1775 22 X Y ID | FMC.py -o P`
  Result:
  ```
  #Longitude Latitude Depth_(km) Strike_A Dip_A Rake_A Strike_B Dip_B Rake_B Seismic_moment_mantissa Exponent_(dyn-cm) X_position(GMT) Y_position(GMT) ID Rupture_type
  -2.54 37.09 12.0 190.925 42.4899 -20.9735 296.709 76.0089 -130.541 9.6045 22.0 X Y ID N-SS
  ```
- Obtaining moment tensor from one nodal plane
  Command:
  `echo -2.54 37.09 12 190.925 42.4899 -20.9735 4.6 X Y ID | FMC.py -i AR -o CMT`
  Result:
  ```
  #Longitude Latitude Depth_(km) mrr mtt mff mrt mrf mtf Exponent_(dyn-cm) X_position(GMT) Y_position(GMT) ID Rupture_type
  -2.54 37.09 12.0 -3.56563 -2.21928 5.78491 6.70126 -1.61249 -5.19047 22.0 X Y ID N-SS
  ```
- Obtaining all the parameters from CMT input file and storing in an ASCII file
  Command:
  `FMC.py -o ALL japan_CMT.dat > Japan_parameters.dat`
- Using CUSTOM output to obtain event location and slip vector of both nodal planes
  Command:
  `echo -2.54 37.09 12 -3.4669 -2.0652 5.5321 6.2368 -1.8004 -5.1775 22 X Y ID | FMC.py -o CUSTOM -of lon,lat,slipA,plungA,slipB,plungB`
  Result:
  ```
  #Longitude Latitude Slip_trend_A Slip_plunge_A Slip_trend_B Slip_plunge_B 2.54 37.09 206.709 -13.9911 100.925 -47.5101
  ```
- Plotting data from input file and shading the symbols with a parameter (Fig. 2)
  Command:
  `FMC.py -p 'Japan 2011 data.png' japan_CMT_2011.dat -pc fclvd`
- Automatic clustering using the position in the Kaverina diagram (default) (Fig. 3)
  `FMC.py -p 'Japan 2011 clusters.png' japan_CMT_2011.dat -cn 0`
- Clustering using the epicentral location (Fig. 4)
  `FMC.py japan_CMT_2011.dat -cn 4 -ci lon,lat`

4. Impact and conclusions

The main research question addressed by FMC is the improvement of the seismotectonic analysis of regions and seismic series. FMC is a powerful tool that allows the user to obtain a deeper insight into the processes responsible for the seismicity, be it natural or human-induced.

With the use of FMC, the user can use a straightforward method to obtain parameters related to the earthquake focal mechanism, especially the double-couple, and can also produce diagrams allowing easy visualization of the DC earthquake rupture mechanisms. The hierarchical clustering analysis is an approximation that is not frequently used in seismotectonics due to its complexity. Its implementation in FMC provides the seismology and seismotectonics communities with a user-friendly tool.

In general, FMC facilitates management of focal mechanism parameters and the implementation of new research approximations to seismicity analysis. To date (see the list of published works in Section 1), the use of the previous version of FMC has improved the quality and clarity of seismotectonic data representation as well as the variety of analyses that can be performed with focal mechanisms, and has provided a basic tool to improve our understanding of the details of tectonic and seismic processes. With the recently implemented clustering algorithm in FMC, seismotectonic analysis will gain a completely new perspective.

FMC is being used by the seismotectonic community, formed by geophysicists, seismologists, earthquake geologists and structural geologists. It has been used in academic research, as well as

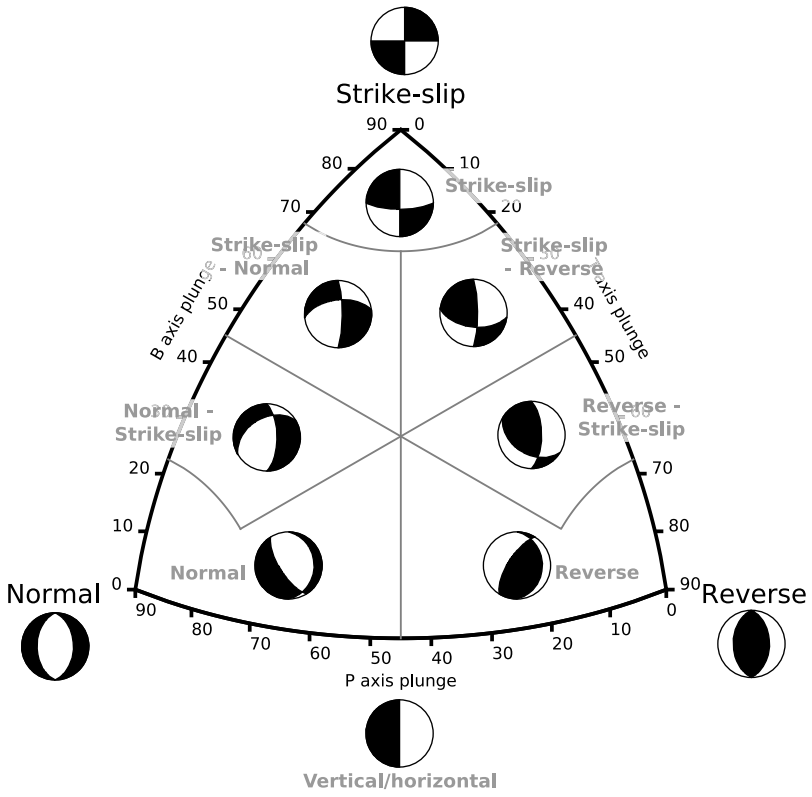

Fig. 1. Diagram for the classification of focal mechanisms used by FMC.

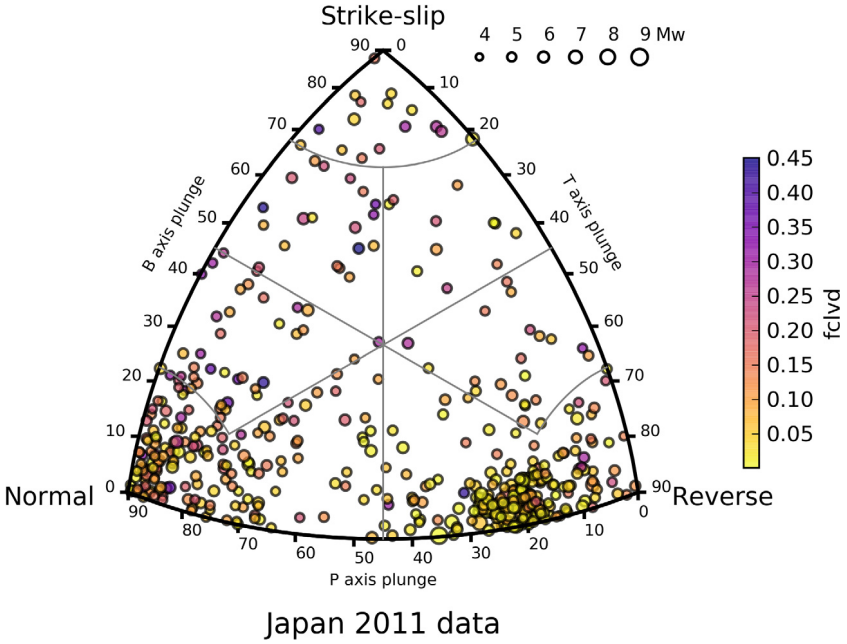

Fig. 2. Plot result from the command "`FMC.py -p 'Japan 2011 data.png' japan_CMT_2011.dat -pc fclvd`".

in seismic and tsunami risk consultancy. It improves the quality of the analysis performed and reduces the time spent on data processing and management.

FMC is growing as a versatile tool that can be implemented easily on automated scripts of data analysis and representation in conjunction with other software suites such as GMT [69] that lack similar tools.

Acknowledgements

I would like to thank Jorge L. Giner Robles, Alberto Jiménez Díaz, Julissa Sanjur, Junqing Liu, Lester Anderson and Andrei Bala, who have tested different versions of the software and suggested improvements for the code. Two anonymous reviewers, and especially R. Myhill, made suggestions to improve the program and the manuscript. This work has been partially supported by the project QuakeStep (CGL2017-83931-C3-1-P) funded by the

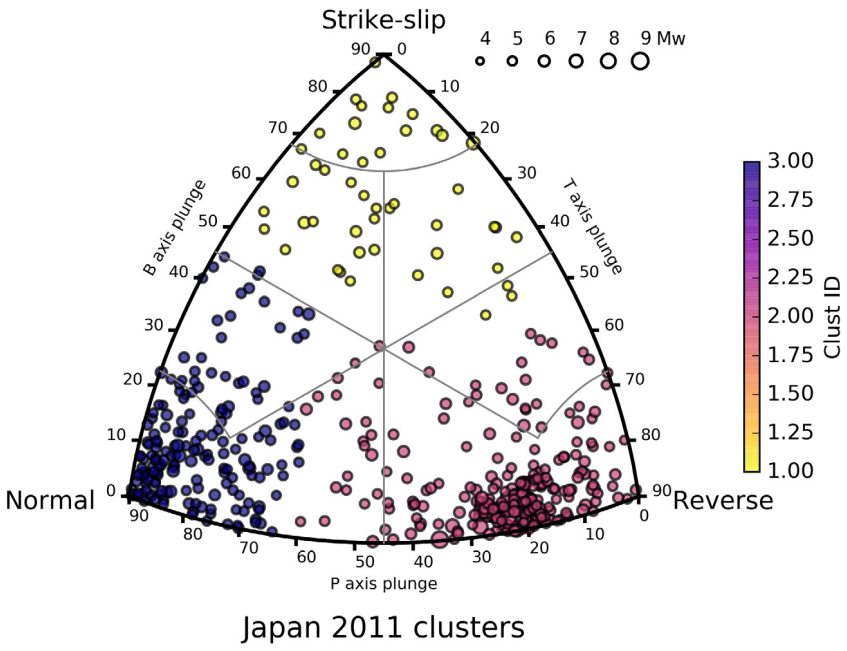

Fig. 3. Plot result from the command "`FMC.py -p 'Japan 2011 clusters.png' japan_CMT_2011.dat -cn 0`".

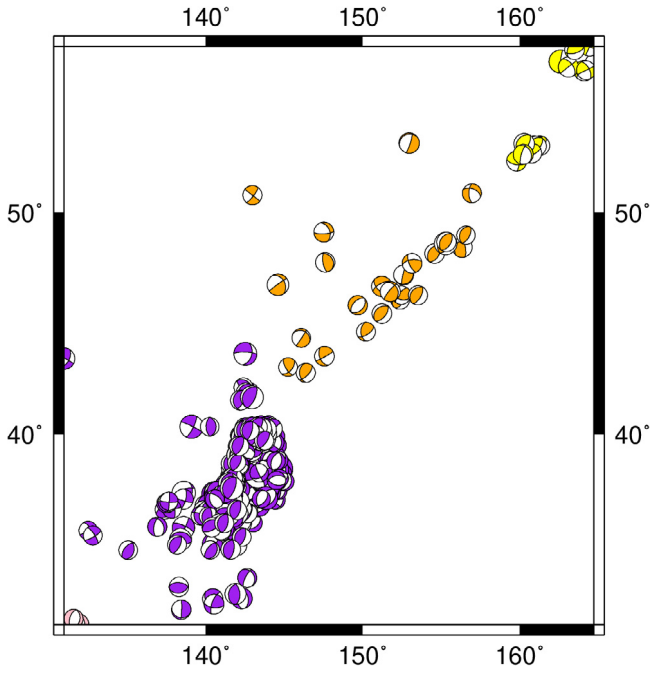

Fig. 4. Plotting with `GMT psmeca` of the clusters obtained with the command "`FMC.py -p 'Japan 2011 spatial clusters.png' japan_CMT_2011.dat -cn 4 -ci lon,lat`".

Ministry of Science, Innovation and Universities of the Spanish Government, Spain.

References

[1] Byerly P. The nature of the first motion in the Chilean earthquake of November 11, 1922. Amer J Sci Ser 1928;5 V(93):232–6.

[2] Byerly P. The earthquake of July 6, 1934: Amplitudes and First Motion. Bull Seismol Soc Am 1938;28(1):1–13.

[3] Koning LPG. On the mechanism of deep focus earthquakes. Gerlands Beitrage z. Geophys 1941;58:159–97.

[4] Honda H, Masatuke A. On the mechanism of the earthquakes and the stresses producing them in Japan and its vicinity. Sci Rep Tohoku Univ 1952;4(1).

[5] Scheidegger AE. The geometrical representation of fault-plane solutions of earthquakes. Bull Seismol Soc Am 1957;47(2):89–110.

[6] Knopoff L. Analytical calculation of the fault-plane problem, vol. 24. Publications of the Dominion Observatory (Ottawa); 1961, p. 309–15.

[7] Langston CA, Helmberger DV. A procedure for modelling shallow dislocation sources*. Geophys J R Astron Soc 1975;42(1):117–30.

[8] Dziewonski AM, Chou T-A, Woodhouse JH. Determination of earthquake source parameters from waveform data for studies of global and regional seismicity. J Geophy Res 1981;86(B4):2825–52.

[9] Benioff H. Orogenesis and deep crustal structure - Additional evidence from seismology. Bull Geol Soc Amer 1954;65(5):385–400. http://dx.doi.org/10.1130/0016-7606(1954)65[385:OADCSE]2.0.CO;2.

[10] Sykes LR. Mechanism of earthquakes and nature of faulting on the mid-oceanic ridges. J Geophys Res 1967;72(8):2131. http://dx.doi.org/10.1029/JZ072i008p02131.

[11] Isacks B, Oliver J, Sykes LR. Seismology and the new global tectonics. J Geophys Res 1968;73(18):5855–99.

[12] Isacks B, Molnar P. Mantle earthquake mechanisms and the sinking of the lithosphere. Nature 1969;223(5211):1121–4.

[13] Frohlich C, Apperson KD. Earthquake focal mechanisms, moment tensors, and the consistency of seismic activity near plate boundaries. Tectonics 1992;11(2):279–96. http://dx.doi.org/10.1029/91TC02888.

[14] Frohlich C, Coffin MF, Massell C, Mann P, Schuur CL, Davis SD, Jones T, Karner G. Constraints on Macquarie Ridge tectonics provided by harvard focal mechanisms and teleseismic earthquake locations. J Geophy Res (1978–2012) 1997;102(B3):5029–41.

[15] Borges JF, Fitas AJS, Bezzeghoud M, Teves-Costa P. Seismotectonics of Portugal and its adjacent Atlantic area. Tectonophysics 2001;331(4):373–87. http://dx.doi.org/10.1016/S0040-1951(00)00291-2.

[16] Igarashi T, Matsuzawa T, Umino N, Hasegawa A. Spatial distribution of focal mechanisms for interplate and intraplate earthquakes associated with the subducting Pacific plate beneath the northeastern Japan arc: A triple-planed deep seismic zone. J Geophys Res 2001;106(B2):2177. http://dx.doi.org/10.1029/2000JB900386.

[17] Ratchkovski NA, Hansen RA. New evidence for segmentation of the Alaska subduction zone. Bull Seismol Soc Am 2002;92(5):1754–65.

[18] Kita S, Okada T, Nakajima J, Matsuzawa T, Hasegawa A. Existence of a seismic belt in the upper plane of the double seismic zone extending in the along-arc direction at depths of 70–100 km beneath NE Japan. Geophys Res Lett 2006;33(24).

[19] Serpelloni E, Vannucci G, Pondrelli S, Argnani A, Casula G, Anzidei M, Baldi P, Gasperini P. Kinematics of the Western Africa-Eurasia plate boundary from focal mechanisms and GPS data. Geophys J Int

2007;169(3):1180–200. http://dx.doi.org/10.1111/j.1365-246X.2007.03367.x.
[20] Frohlich C. Display and quantitative assessment of distributions of earthquake focal mechanisms. Geophys J Int 2001;144(2):300–8. http://dx.doi.org/10.1046/j.1365-246x.2001.00341.x.
[21] Kagan YY. Double-couple earthquake focal mechanism: Random rotation and display. Geophys J Int 2005;163(3):1065–72. http://dx.doi.org/10.1111/j.1365-246X.2005.02781.x.
[22] Kaverina AN, Lander AV, Prozorov AG. Global creepex distribution and its relation to earthquake-source geometry and tectonic origin. Geophys J Int 1996;125(1):249–65.
[23] Snoke JA. A program for focal mechanism determination by combined use of polarity and SV-P amplitude ratio data. Earthquake Notes 1984.
[24] Johnson CE, Bittebinder A, Bogaert B, Dietz L, Kohler W. Earthworm: A flexible approach to seismic network processing. Iris Newslett 1995;14(2):1–4.
[25] Creager K. Coral. Seismol Res Lett 1997;68(2):269–71.
[26] Louvari EK, Kiratzi AA. RAKE: A windows program to plot earthquake focal mechanisms and the orientation of principal stresses. Comput Geosci 1997;23(8):851–7. http://dx.doi.org/10.1016/S0098-3004(97)00070-8.
[27] Lees JM. Geotouch: software for three and four dimensional GIS in the earth sciences. Comput Geosci 2000;26(7):751–61. http://dx.doi.org/10.1016/S0098-3004(99)00133-8.
[28] Gasperini P, Vannucci G. FPSPACK: A package of FORTRAN subroutines to manage earthquake focal mechanism data. Comput Geosci 2003;29(7):893–901. http://dx.doi.org/10.1016/S0098-3004(03)00096-7.
[29] Srivastava NN, Thakor RU, Patel SV, Viroja SG, Chetta US, Sharma SA. Construction of beachball diagram using java-based software application "dishansh 2005". Seismol Res Lett 2006;77(5):554–8. http://dx.doi.org/10.1785/gssrl.77.5.554, https://pubs.geoscienceworld.org/srl/article/77/5/554-558/143275.
[30] Luis JF. Mirone: A multi-purpose tool for exploring grid data. Comput Geosci 2007;33(1):31–41. http://dx.doi.org/10.1016/j.cageo.2006.05.005.
[31] Labay KA, Haeussler PJ. 3D visualization of earthquake focal mechanisms using ArcScene - ScienceBase-catalog. In: ScienceBase-catalog, data series, vol. 241. USGS; 2007, https://www.sciencebase.gov/catalog/item/53cd492de4b0b290850eef1c.
[32] Scherbaum F, Kuehn N, Zimmermann B. Earthquake focal mechanism - Wolfram demonstrations project. 2009, http://demonstrations.wolfram.com/EarthquakeFocalMechanism/.
[33] Hanka W, Saul J, Weber B, Becker J, Harjadi P, Fauzi, GITEWS Seismology Group. Real-time earthquake monitoring for tsunami warning in the Indian Ocean and beyond. Nat Hazards Earth Syst Sci 2010;10(12):2611–22. http://dx.doi.org/10.5194/nhess-10-2611-2010, http://www.nat-hazards-earth-syst-sci.net/10/2611/2010/.
[34] Krieger L, Heimann S. Mopad–moment tensor plotting and decomposition: a tool for graphical and numerical analysis of seismic moment tensors. Seismol Res Lett 2012;83(3):589–95. http://dx.doi.org/10.1785/gssrl.83.3.589, https://pubs.geoscienceworld.org/srl/article/83/3/589-595/143981.
[35] Herrmann RB. Computer programs in seismology: an evolving tool for instruction and research. Seismol Res Lett 2013;84(6):1081–8. http://dx.doi.org/10.1785/0220110096, https://pubs.geoscienceworld.org/srl/article/84/6/1081-1088/315307.
[36] Conder J. focalmech - File Exchange - MATLAB Central. 2017, https://es.mathworks.com/matlabcentral/fileexchange/61227-focalmech-fm-centerx-centery-diam-varargin.
[37] Heimann S, Isken M, Kühn D, Sudhaus H, Steinberg A, Daout S, Cesca S, Vasyura-Bathke H, Dahm T. Grond - A probabilistic earthquake source inversion framework. In: GFZ data services. 2018, http://dx.doi.org/10.5880/GFZ.2.1.2018.003, http://dataservices.gfz-potsdam.de/panmetaworks/showshort.php?id=escidoc:3600903.
[38] CERI. bb matlab function. The Center for Earthquake Research and Information - The University of Memphis; 2019, https://www.memphis.edu/ceri/.
[39] Helffrich G. Focal mechanisms. In: ELSI. 2019, https://members.elsi.jp/~george/focmec.html.
[40] Patau G. PSMECA (GMT). In: SOEST Hawaii. 2019, https://www.soest.hawaii.edu/gmt/gmt/html/man/psmeca.html.
[41] Bernardi F. PyTDMT - Python time domain moment tensor. In: INGV. 2019.
[42] Lister G. eQuakes. ANU Research School of Earth Sciences; 2010, http://rses.anu.edu.au/tectonics/equakes/.
[43] Khalil AR, Al-Arifi NS. Focal mechanisms overview. Earth Sci Inform 2018;1–8. http://dx.doi.org/10.1007/s12145-018-0367-1.
[44] Frohlich C. Triangle diagrams: ternary graphs to display similarity and diversity of earthquake focal mechanisms. Phys Earth Planet Inter 1992;75(1–3):193–8. http://dx.doi.org/10.1016/0031-9201(92)90130-N.
[45] Lana X, Fernández Mills G. Local lithospheric stress distribution deduced by means of the total inversion algorithm and an objective classification method. Pure Appl Geophys PAGEOPH 1992;138(2):229–47. http://dx.doi.org/10.1007/BF00878897.
[46] Kumar M, Rao N, Chalam SV. A seismotectonic study of the Burma and Andaman arc regions using centroid moment tensor data. Tectonophysics 1996;253(1–2):155–65. http://dx.doi.org/10.1016/0040-1951(95)00027-5.
[47] Tranos MD. Tr method: a practical tool to analyze focal mechanisms and identify the 'real' seismogenic fault of an extensional or compressional shallow earthquake sequence. Tectonophysics 2014;633:77–97. http://dx.doi.org/10.1016/J.TECTO.2014.06.027.
[48] Vavryčuk V. Moment tensor decompositions revisited. J Seismol 2015;19(1):231–52. http://dx.doi.org/10.1007/s10950-014-9463-y.
[49] Hudson JA, Pearce RG, Rogers RM. Source type plot for inversion of the moment tensor. J Geophys Res 1989;94(B1):765. http://dx.doi.org/10.1029/JB094iB01p00765.
[50] Willemann RJ. Cluster analysis of seismic moment tensor orientations. Geophys J Int 1993;115(3):617–34. http://dx.doi.org/10.1111/j.1365-246X.1993.tb01484.x.
[51] Myhill R. Slab buckling and its effect on the distributions and focal mechanisms of deep-focus earthquakes. Geophys J Int 2013;192(2):837–53. http://dx.doi.org/10.1093/gji/ggs054.
[52] Cesca S, Şen AT, Dahm T. Seismicity monitoring by cluster analysis of moment tensors. Geophys J Int 2014;196(3):1813–26. http://dx.doi.org/10.1093/gji/ggt492.
[53] Lister GS, Forster MA, Muston JE, Mousavi S, Hejrani B. Structural geology and the seismotectonics of the 2004 great sumatran earthquake. Tectonics 2018;37(11):4101–19. http://dx.doi.org/10.1002/2017TC004708.
[54] Chen X, Wang R, Huang W, Jiang Y, Yin C. Clustering-based stress inversion from focal mechanisms in microseismic monitoring of hydrofracturing. Geophys J Int 2018;215(3):1887–99. http://dx.doi.org/10.1093/gji/ggy388.
[55] Álvarez-Gómez JA, Aniel-Quiroga Í, González M, Olabarrieta M, Carreño E. Scenarios for earthquake-generated tsunamis on a complex tectonic area of diffuse deformation and low velocity: The Alboran Sea, Western Mediterranean. Marine Geol 2011;284(1–4):55–73.
[56] Álvarez-Gómez JA, Gutiérrez Gutiérrez OQ, Aniel-Quiroga Í, González M. Tsunamigenic potential of outer-rise normal faults at the Middle America trench in Central America. Tectonophysics 2012;574–575:133–43.
[57] Custódio S, Lima V, Vales D, Cesca S, Carrilho F. Imaging active faulting in a region of distributed deformation from the joint clustering of focal mechanisms and hypocentres: Application to the Azores–western Mediterranean region. Tectonophysics 2016;676:70–89.
[58] Alonso-Henar J, Álvarez-Gómez JA, Martínez-Díaz JJ. Neogene-quaternary evolution from transpressional to transtensional tectonics in Northern Central America controlled by cocos: Caribbean subduction coupling change. J Iberian Geol 2017;43(3):519–38. http://dx.doi.org/10.1007/s41513-017-0034-2.
[59] Fontiela J, Sousa Oliveira C, Rosset P. Characterisation of seismicity of the azores archipelago: an overview of historical events and a detailed analysis for the period 2000–2012. In: Volcanoes of the Azores. Berlin, Heidelberg: Springer; 2018, p. 127–53.
[60] Staller A, Álvarez-Gómez JA, Luna MP, Béjar-Pizarro M, Gaspar-Escribano JM, Martínez-Cuevas S. Crustal motion and deformation in Ecuador from cGNSS time series. J South Amer Earth Sci 2018;86:94–109. http://dx.doi.org/10.1016/J.JSAMES.2018.05.014.
[61] Bălă A, Radulian M, Popescu E, Toma-Danilă D. Catalogue of earthquake mechanism and correlation with the most active seismic zones in south-eastern part of romania. In: Seismic Hazard and Risk Assessment. Cham: Springer; 2018, p. 23–37. http://dx.doi.org/10.1007/978-3-319-74724-8.
[62] Pan Z, He J, Li J. Contemporary crustal deformation within the pamir plateau constrained by geodetic observations and focal mechanism solutions. Pure Appl Geophys 2018;175(10):3463–84. http://dx.doi.org/10.1007/s00024-018-1872-3.
[63] Illsley-Kemp F, Keir D, Bull JM, Gernon TM, Ebinger C, Ayele A, Hammond JOS, Kendall J-M, Goitom B, Belachew M. Seismicity during continental breakup in the red sea rift of northern afar. J Geophy Res 2018;123(3):2345–62. http://dx.doi.org/10.1002/2017JB014902.
[64] Radulian M, Bala A, Popescu E, Toma-Danila D, Toma-Danila D. Earthquake mechanism and characterization of seismogenic zones in south-eastern part of Romania. Ann Geophys 2018;61(1):SE108. http://dx.doi.org/10.4401/ag-7443.
[65] Álvarez-Gómez JA, Martin R, Pérez-López R, Stich D, Cantavella JV, Martínez-Díaz JJ, Morales Soto J, Martínez-García P, Soto JI, Carreño E. La serie sísmica de Alhucemas 2016. Partición de la deformación e interacción de estructuras en un límite de placas difuso. Geo-Temas 2016;16(2):491–4.

[66] Quinones LA, DeShon HR, Magnani MB, Frohlich C. Stress orientations in the Fort Worth Basin, Texas, determined from earthquake focal mechanisms. Bull Seismol Soc Am 2018;108(3A):1124–32. http://dx.doi.org/10.1785/0120170337.

[67] Rubinstein JL, Ellsworth WL, Dougherty SL. The 2013–2016 induced earthquakes in harper and sumner counties, Southern Kansas. Bull Seismol Soc Am 2018;108(2):674–89. http://dx.doi.org/10.1785/0120170209.

[68] Popescu E, Radulian M, Bala A, Toma-Danila D. Earthquake mechanism in the Vrancea subcrustal source and in the adjacent crustal seismogenic zones of the south-eastern Romania. Romanian Rep Phys 2018;704.

[69] Wessel P, Smith WHF, Scharroo R, Luis J, Wobbe F. Generic mapping tools: improved version released. EOS Trans Am Geophys Union 2013;94(45):409–10. http://dx.doi.org/10.1002/2013EO450001.

[70] Aki K, Richards PG. Quantitative seismology, theory and methods, vol. I and II. San Francisco: W. H. Freeman; 1980.

[71] Johnston AC, Coppersmith KJ, Kanter LR, Cornell CA. The earthquakes of stable continental regions. Volume 1: Assessment of large earthquake potential. In: EPRI, editor. Electric Power Research Institute; 1994, p. 370.

[72] Triep EG, Sykes LR. Catalog of shallow intracontinental earthquakes (Triep, 1996). 1996, https://www.ldeo.columbia.edu/seismology/triep/intra.expl.html.

[73] Célérier B. Remarks on the relationship between the tectonic regime, the rake of the slip vectors, the dip of the nodal planes, and the plunges of the P, B, and T axes of earthquake focal mechanisms. Tectonophysics 2010;482(1–4):42–9. http://dx.doi.org/10.1016/j.tecto.2009.03.006, http://dx.doi.org/10.1016/j.tecto.2009.03.006.

[74] Tape W, Tape C. A geometric setting for moment tensors. Geophys J Int 2012;190(1):476–98. http://dx.doi.org/10.1111/j.1365-246X.2012.05491.x.

[75] Aso N, Ohta K, Ide S. Mathematical review on source-type diagrams. Earth Planets Space 2016;68(1):52. http://dx.doi.org/10.1186/s40623-016-0421-5.

[76] Ekström G, Nettles M, Dziewoński AM. The global CMT project 2004-2010: Centroid-moment tensors for 13,017 earthquakes. Phys Earth Planet Inter 2012;200–201:1–9. http://dx.doi.org/10.1016/j.pepi.2012.04.002.